

ANALYSIS OF ROGOWSKI COIL BEHAVIOR UNDER NON IDEAL MEASUREMENT CONDITIONS

G. Crotti ¹, D. Giordano ¹, A. Morando ²

¹ Istituto Nazionale di Ricerca Metrologica (INRiM), Torino, Italy, g.crotti@inrim.it, d.giordano@inrim.it

² Dipartimento di Ingegneria Elettrica, Politecnico di Torino, Italy, andrea.morando@polito.it

Abstract – This work illustrates an analysis of Rogowski coils for power applications, when operating under non ideal measurement conditions. The developed numerical model, validated by comparison with other methods and experiments, enables to investigate the effects of the geometrical and constructive parameters on the measurement behavior of the coil.

Keywords: Rogowski coil, numerical models, Biot-Savart.

1. INTRODUCTION

The Rogowski coil is a current transducer which is often used in electrical power applications to measure sinusoidal low frequency and transient currents [1]. Its properties of linearity, ease of installation and lightness allow its use as a good alternative to conventional transducers, such as the current transformers and the shunts.

The measurement uncertainty of the Rogowski coils can significantly vary, as a function of the construction characteristics and the measurement conditions, ranging from some percent to the part per thousand. Optimization of their behavior is usually performed experimentally on coil prototypes [2]. Modelling approaches [1,3-5] have been developed which allow the prediction of the transducer behavior under ideal measurement conditions such as:

- circular coil shape;
- power conductor of infinite length and thin cross-section;
- power conductor placed in the coil centre;
- power conductor axis orthogonal to the coil plane;
- winding cross-section of rectangular shape;
- coil turns uniformly distributed along a whole circumference (closed coil).

The paper describes a numerical tool which has been developed to allow the analysis of the Rogowski coils under non ideal conditions, by varying both the circuital and coil geometrical parameters. The modelling approach and its validation are briefly described. Examples of application are given, which show how the model can be used in the design phase to predict and improve the Rogowski coil measurement accuracy.

2. ANALYSIS PROCEDURE

The Rogowski coil is essentially a linear mutual inductor, linked with the magnetic field lines generated by the current $i(t)$ (i.e. the measurand), which flows in the power conductor (primary conductor). The electro-motive force $e(t)$ induced in the coil is given by:

$$e(t) = M \frac{di(t)}{dt} \quad (1)$$

where M is the mutual inductance coefficient between the coil and the primary conductor.

Assuming a closed coil ideally wound with a continuous turn distribution, with a small cross-sectional area and in no-load electrical operating conditions, the mutual inductance is a constant term, because, according to the Ampere's law, the magnetic flux linked with the coil is independent of the position of the primary conductor within the closed coil.

In the following, the variations of the mutual inductance M (or, equally, of the magnetic flux per-unit current) are analysed, which are consequent to the deviation from the ideal hypothesis previously indicated.

The analysis is performed by considering a flexible and openable Rogowski coil, composed of circular turns, with the following geometrical features:

$$N = 130; R_e = 175 \text{ mm}; R_i = 150 \text{ mm}; d = 2 \text{ mm}$$

where N is the number of coil turns, R_e and R_i are respectively the external and the internal coil radius and d is the conductor diameter of the winding.

The input and output terminals of the coil are usually not geometrically coincident and the gap between them is quantified by the opening angle β (Fig. 1). The coil terminals are assumed to be connected to an impedance of ideally infinite value (e.g. the input impedance of a voltmeter instrument), so that the presence of induced currents in the coil can be disregarded.

In order to investigate the most important constructive and geometrical parameters, a 3D modelling approach is employed. The attention is focused on the use of this model, which deduces the magnetic vector potential distribution through the Biot-Savart's law.

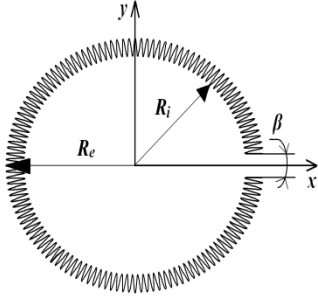


Fig. 1 : Geometrical features of the Rogowski coil.

The calculation of the magnetic flux linked with the coil is then performed through the line integral of the magnetic potential vector along the coil turns. A two-dimensional (2D) model, based on the Finite Element Method (FEM), is also used to validate the 3D results.

The modelling analysis allows the quantification of the behavior of a Rogowski coil as a function of the:

- positions of the power conductor with respect to the coil centre;
- opening angle β values;
- coil eccentricity;
- non-orthogonal orientation of the primary conductor axis with respect to the coil plane;

Moreover the following issues can be handled:

- influence of external magnetic field sources;
- presence of a compensation turn or a counter-wound coil;
- non-uniform distribution of the turns along the coil;
- different shapes of the primary conductor (circular and bar-type).

Some results obtained by the model are compared with experiments performed in the high current laboratory of the Istituto Nazionale di Ricerca Metrologica (INRiM) of Torino by using a commercial Rogowski coil.

3. MODELLING AND EXPERIMENTAL APPROACHES

3.1. Numerical models

The 3D model is developed by computing the magnetic potential vector per-unit current \vec{A} , through the Biot-Savart's law. The linked flux and the mutual inductance M with the coil are then evaluated by integrating the magnetic potential along the coil turns.

First, the vector potential \vec{A} is calculated according to the relationship:

$$\vec{A} = \frac{\mu_0}{4\pi} \int_{\ell} \frac{d\vec{l}}{\rho} \quad (2)$$

where $\mu_0 = 4\pi \cdot 10^{-7}$ H/m is the absolute magnetic permeability of the empty space, ρ is the distance between the field source and the computational point in the coil, ℓ is the length of the primary conductor. The mutual inductance coefficient is then computed, thanks to the Stokes' theorem, as:

$$M = \int_{\Gamma} \vec{A} \cdot d\vec{\gamma} \quad (3)$$

where Γ is the coil helical profile. Equations (2) and (3) are handled numerically. A preliminary evaluation of the weight of the discretization steps is carried out, in order to obtain reliable results. To this end, several values of the primary conductor length and of the coil turn elementary divisions are considered. A conductor length of 22 m and 800 divisions per turn are adopted in the following investigations. A further increase of the conductor length and of the turn divisions does not modify appreciably the results.

An helical winding is built according to the following equation system, defined according to the Cartesian reference system xyz (see Fig. 2), centered in the coil centre:

$$\begin{cases} x = [r \cdot \cos\gamma + R] \cdot \cos\theta \\ y = [r \cdot \cos\gamma + R] \cdot \sin\theta \\ z = r \cdot \sin\gamma \end{cases} \quad (4)$$

where R is the average coil radius, r the turn radius, θ the angle in the x - y plane and γ the angle in the y' - z' plane, defined according to the local coordinates $x'y'z'$ which refer to a single turn.

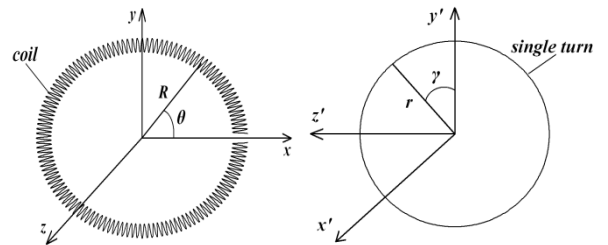


Fig. 2: Reference system for the coil building.

The relations (4) allow the description of a Rogowski coil made of: a) a single winding; b) a single winding plus a compensation turn and c) a winding with a counter-wound compensation winding.

The results obtained with the 3D model are validated by comparison with the values computed with a FEM model. The 2D FEM model is based on a magnetic potential vector weak formulation, which uses a meshing technique with triangular elements and first order shape functions.

Table 1 shows the comparison between the results obtained with the two methods, where the mutual inductance values refer to a coil with the circular shape primary conductor in centred position. Under this hypothesis, the flux linked with the coil can be also analytically computed.

Table 1: Comparison between the 3D, 2D and analytical computations.

| Computation | Linked magnetic flux (nWb) |
|----------------------|----------------------------|
| 3D Biot-Savart model | 78.6470 |
| FEM | 78.2131 |
| Analytical | 78.2139 |

A deviation of about 0.5 % is found between the result obtained by the 3D model and those computed analytically and by FEM. This deviation can be explained by considering that in the FEM and in the analytical computation a continuous turn distribution is considered, while in the 3D analysis the magnetic flux is linked with the actual coil helix.

3.2. Experimental set-up

The measurements are carried out under sinusoidal supply at power frequency, feeding a Y-bar system which is adopted to minimize the stray magnetic fields produced by the current flowing in the main circuit. The standard current transformer (CT) is placed at one of the Y-system terminals, the Rogowski coil at the other one. The mutual inductance value is deduced from the ratio of the rms value of the measured voltage (from the Rogowski coil integrator output, V_{coil}) to the rms current measured by the CT ($V_{ct,r}/R$). The generation and measurement systems are schematically presented in Fig. 3.

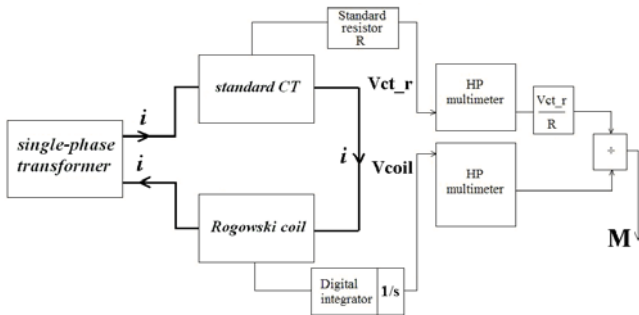


Fig. 3: Scheme of the experimental set-up.

The flexible coil with a primary conductor of rectangular section and the power circuit are shown in Fig. 4a) and 4b), respectively.

4. RESULTS AND DISCUSSION

The results presented in the following are normalized to the reference value M_0 which is the mutual inductance under ideal conditions (centred primary conductor and closed coil).

In the first tests, a primary conductor of circular shape is displaced with respect to the coil centre along the x-axis (Fig. 1), having assumed different values of the opening

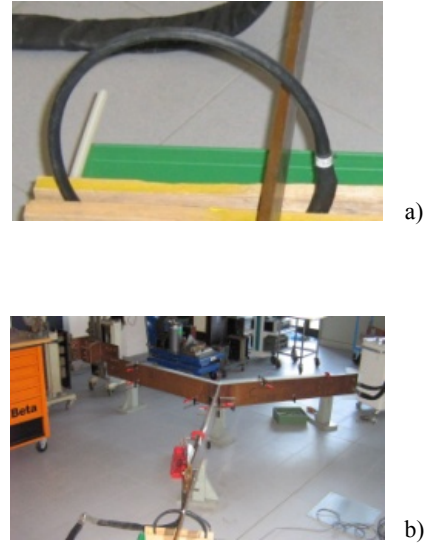


Fig. 4: Experimental setup: a) Rogowski coil with primary conductor displaced with respect to the coil center b) test power circuit.

value β . As expected, the deviation ΔM of the normalized mutual inductance from unity is significant when the conductor is close to the coil terminals, where the gap causes a decrease of the mutual inductance (see Fig. 5a). This deviation increases with the opening angle β (see Fig. 5b).

The model also enables to analyse the effects of a non-uniform coil turn distribution. The helical coil description is carried out by assigning a weight (p) to the coil pitch of each single turn. Some turn pitches are assigned by the user and the others are consequently recomputed with a uniform weight. By defining m as the number of the turns whose pitch is modified and concentrating these turns in proximity to the coil terminals, the influence of the primary conductor displacements on the mutual inductance is, as expected, strongly reduced. The improved turn configuration, that allows the minimization of the deviation of the mutual inductance with respect to the reference value, clearly depends on the air gap between the coil terminals; in fact, the number of turns, whose pitch is modified, increases with the β angle value.

Fig. 6 shows the normalized mutual inductance as a function of the distance of the primary conductor from the coil centre with an improved turn distribution ($p = 0.9$, $m = m_T$). The deviation values are compared with those obtained with a uniform turn distribution, which are reported in brackets.

An improved turn distribution plays an important role in the compensation of the effects due to an external magnetic field source. Fig. 7 shows the behavior of the mutual inductance of a coil when a linear current-carrying conductor (e.g. a return conductor carrying the same current) is placed parallel to the primary conductor, at a distance D from the coil centre. The numerical values are compared by adopting both a uniform and a non-uniform turn distributions. The reduction of the deviation, as a function of

the position of the primary conductor with respect to the coil centre, is very significant (see Fig. 7).

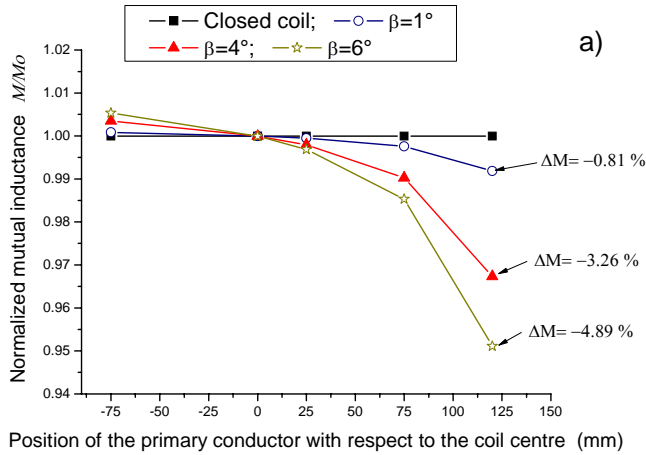


Fig. 5: Behavior of the normalized mutual inductance as a function of: a) the primary conductor position, b) the opening angle β .

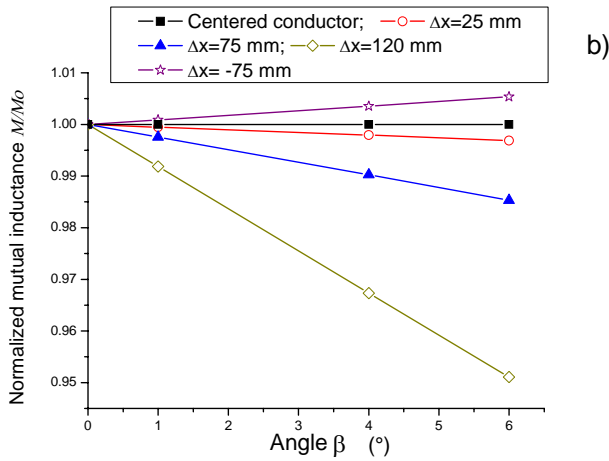


Fig. 6: Normalized mutual inductance behavior, with improved turn distributions. Values in brackets are obtained with a uniform turn distribution.

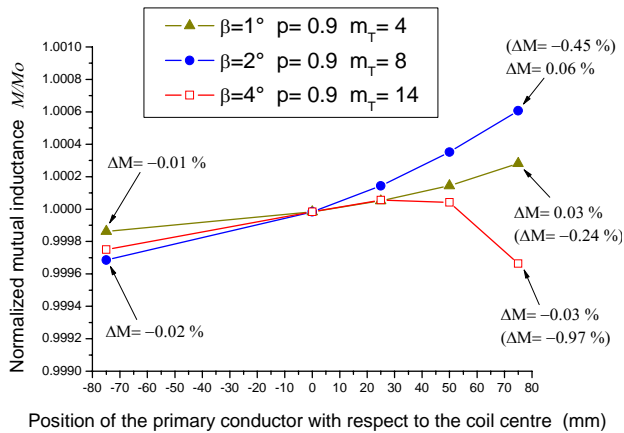


Fig. 7: Effects on the mutual inductance of a return conductor, with a uniform and a non-uniform turn distribution.

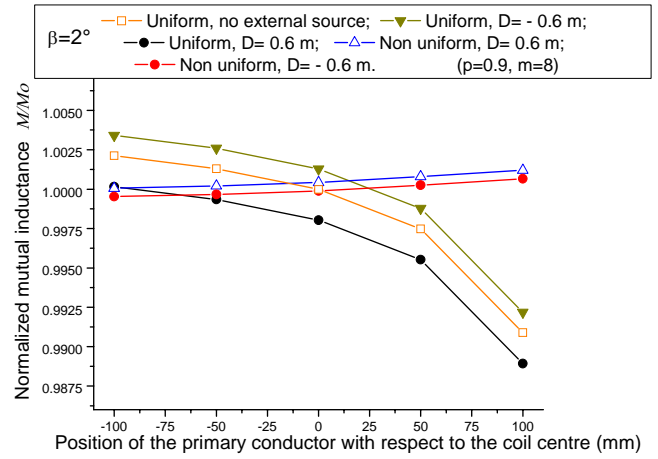


Fig. 8: Normalized mutual inductance behavior with elliptical coils.

To analyse the influence of a non-circular shape of the coil, two elliptical shapes are investigated with different eccentricity values ($e = 0.45$ and $e = 0.68$), where the parameter e is defined by considering the major axis of the ellipse along the x -axis (Fig. 8).

The comparison between the studied cases is plotted in Fig. 8 where the mutual inductance varies as a function of the horizontal position of the circular primary conductor. The eccentricity effect increases the deviation with respect to the circular shape when the conductor is a few centimetres away the centre.

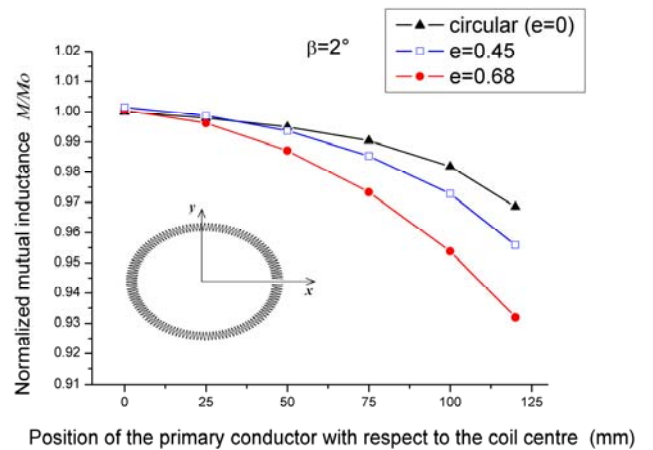


Fig. 9: well clarifies how the flux generated by the external conductor links the entire coil circumference inducing an additional electromotive force. The final effect is an uncorrected indication of the current value to be measured. In order to quantify this discrepancy,

As well known, the behavior of the Rogowski coil is significantly affected by the presence of external fields having components along the coil axis (z -axis), as those generated by conductors which lay in the same plane of the device. As an example, Fig. 9 well clarifies how the flux generated by the external conductor links the entire coil circumference inducing an additional electromotive force. The final effect is an uncorrected indication of the current value to be measured. In order to quantify this discrepancy,

a unitary current is considered, which flows in the conductor posed in the coil plane, at a distance D from the coil centre, when the same current is assumed in the main conductor (see Fig. 9).

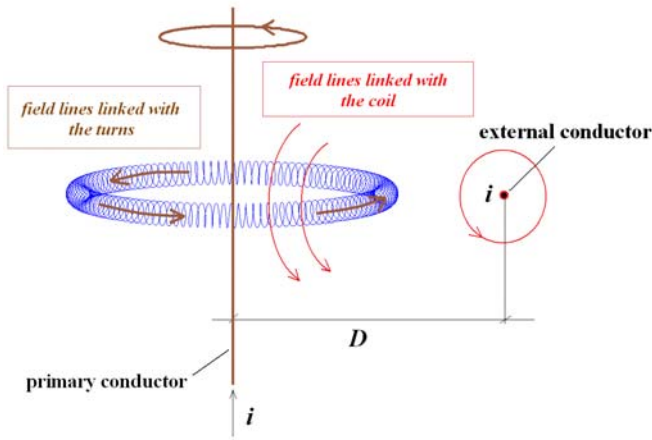


Fig. 9: Influence of an external conductor on the coil measurement.

If the current which flows in the primary and in the external conductor is equal to 1 A, the influence of the external source can be quantified by considering an equivalent current which, flowing in the primary conductor (in absence of the external one), should generate the same magnetic flux totally linked by the coil. In the first column of Table 2, the strong influence of the external field is put in evidence. A compensation turn, wound in the opposite direction with respect to the main coil, or a second winding, with the same number of turns wound in the opposite direction with respect to the main one [6], are efficiently used for the compensation of the effects due to the external field having components along the coil axis (z -axis). Rogowski coils with a compensation turn and of a double coil with a counter-wound winding are illustrated, respectively, in Fig. 10a) and Fig. 10b).

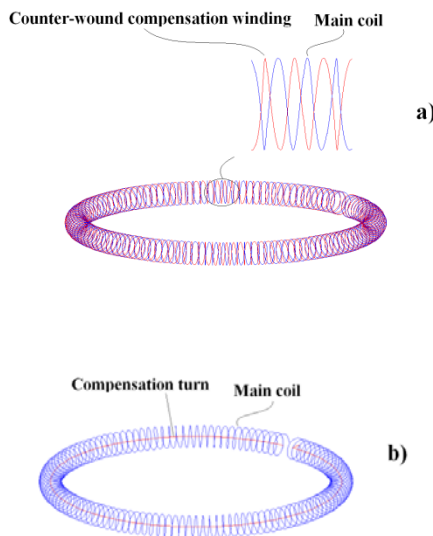


Fig. 10: Plotting of the coil with a) a counter-wound winding, b) a compensation turn.

Table 2 quantifies the advantages deriving from adding a compensation turn and a counter-wound compensation winding to a single coil, with a linear conductor placed at the distance D from the coil centre. The influence of the external field is reduced of more than two orders of magnitude. In particular, the compensation with a counter-wound winding, with the same number of turns of the main coil, reduces the deviation from the unitary current value to about $1 \cdot 10^{-5}$.

Table 2: Effects of the compensation turn and of the counter-wound coil on a transversal magnetic field expressed through the equivalent current.

| | <u>SINGLE COIL</u> | <u>SINGLE COIL+COMPENSATION TURN</u> | <u>SINGLE COIL+COUNTER-WOUND COMPENSATION WINDING</u> |
|-----------|--------------------|--------------------------------------|---|
| $D=0.4$ m | 1.5525 A | 1.0017 A | 1 A |
| $D=0.7$ m | 1.3060 A | 1.0008 A | 1 A |

The effects of the non-orthogonal positioning of the primary conductor axis with respect to the coil plane are then investigated. The analysis is carried out by considering several values of the tilt angle α , for different coil gaps. Fig. 11 shows that an anti-symmetrical behavior occurs for positive and negative α values.

This effect can be considerably reduced by adopting a counter-wound winding, because the magnetic field, generated by the tilted primary conductor, introduces also field components along the coil axis. By using the double coil, the influence of the angle α decreases of about one order of magnitude, as shown in Fig. 12.

As last analysis, a primary conductor with a rectangular cross-section is considered, modelling the bulk conductor with a number of thin conductors suitably positioned and assuming the opening angle $\beta = 2^\circ$.

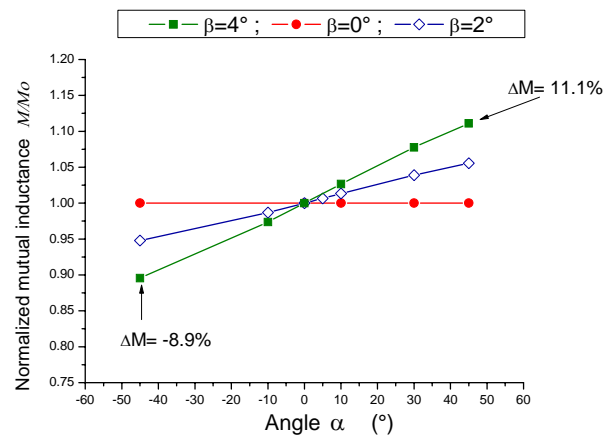


Fig. 11: Normalized mutual inductance behavior with non-orthogonal position of the primary conductor.

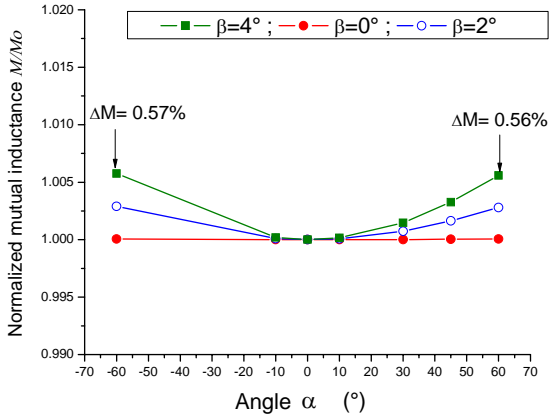


Fig. 12: Normalized mutual inductance behavior in non-orthogonal conditions: effect of the addition of a second winding.

The numerical results are compared with those measured, by using a commercial Rogowski coil, whose main constructive parameters are only partially known. Fig. 13 compares the measured values with those obtained by the model, with the assumption of uniform turn distribution. A maximum relative deviation of about 0.2% has been obtained (Fig. 13), which can be partially explained by taking into account both the uncertainty in the estimation of the geometrical and constructive parameters and the model numerical approximation. However, the agreement between the experiments and the model results can be improved by simulating a concentration of the turns in correspondence to the coil terminals ($m_T = 8, p = 0.9$). Under this condition, the relative deviation with respect to the reference value, when the primary conductor is positioned at 85 mm from the coil centre, is less than one part per thousand.

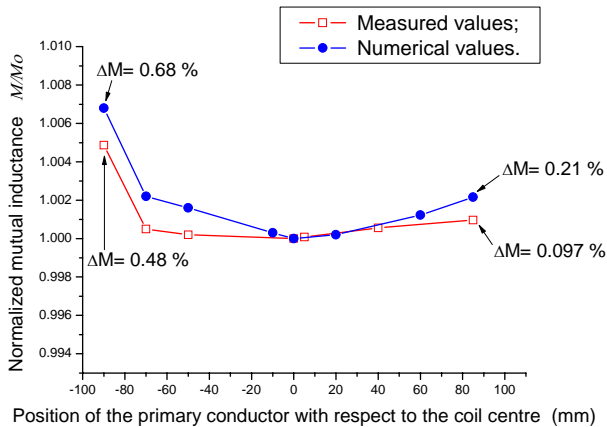


Fig. 13: Comparison between the measured and the model results, with a bar-type primary conductor.

5. CONCLUSIONS

A 3D modeling approach has been presented, which allows the prediction of the Rogowski coil behavior under non ideal measurement operations. The adopted model, validated by the comparison with other methods and

experiments, has been applied to the analysis under steady-state supply conditions at power frequency.

Through the use of the developed models, the design parameters (e.g. a non-uniform turns distribution and the addition of a second winding) can be improved. The models also allow the identification of the best solutions, as regards the measurement circuit arrangement, taking into account the constraints of the actual operating conditions.

REFERENCES

- [1] J. D. Ramboz, "Machinable Rogowski Coil, Design, and Calibration", *IEEE Transactions on Instrumentation and Measurement*, vol. 45, no. 2, pp. 511-515, April 1996.
- [2] Kang-Won Lee, Jeong-Nam Park, Seong-Hwa Kang, Yong-Shin Lee, Gil-Ho Ham, Yong-Mu Jang, Kee-Joe Lim, "Geometrical effects in the current measurement by Rogowski sensor", *Proc. International Symposium on Electrical Insulating Materials*, Nov. 2001.
- [3] M. Bombonato, D. D'Amore, "A classical device for the modern measurements: the Rogowski coil", "Un componente classico per le misure moderne: la bobina di Rogowski", *L'Elettrotecnica*, vol. LXXVI, no. 9, pp. 765-771, Sept. 1989.
- [4] D.A. Ward, J.L.T. Exon, "Using Rogowski coils for transient current measurements", *Engineering Science and Educational Journal*, vol. 2, pp. 105-113, June 1993.
- [5] J. Hlavacek, R. Prochazka, K. Draxler, V. Kvasnicka, "The Rogowski coil design software", *Proc. 16th IMEKO TC4 International Symposium*, Firenze, 2008, pp. 295-300, ISBN 978-88-903149-3-3.
- [6] C.D.M. Oates, A. J. Burnett, C. James, "The design of high performance Rogowski coils", *Power Electronics, Machines and Drives*, pp. 568-572, April 2002.
- [7] M. Rezaee, H. Heydari, "Mutual inductances comparison in Rogowski coil with circular and rectangular cross-sections and its improvement", *Proc. 3rd IEEE Conference on Industrial Electronics and Applications*, pp. 1507-1511, June 2008.